NeuroImage: Clinical 24 (2019) 101963

Contents lists available at ScienceDirect

NeuroImage: Clinical

journal homepage: www.elsevier.com/locate/ynicl

Widespread white matter connectivity abnormalities in narcolepsy type 1: A diffusion tensor imaging study

Jari K. Gool[a,b,c,*], Rolf Fronczek[b,c], Alexander Leemans[d], Dennis A. Kies[e], Gert Jan Lammers[b,c], Ysbrand D. Van der Werf[a]

[a] Department of Anatomy and Neurosciences, Amsterdam UMC (Location VUmc), Amsterdam, the Netherlands
[b] Sleep-Wake Centre, Stichting Epilepsie Instellingen Nederland (SEIN), Heemstede, the Netherlands
[c] Department of Neurology, Leiden University Medical Center, Leiden, the Netherlands
[d] Image Sciences Institute, University Medical Center Utrecht, Utrecht, the Netherlands
[e] Department of Radiology, Leiden University Medical Center, Leiden, the Netherlands

ARTICLE INFO

Keywords:
Disorders of excessive somnolence
Narcolepsy
Hypocretin
Magnetic resonance imaging
Diffusion tensor imaging
White matter

ABSTRACT

Narcolepsy type 1 is caused by a selective loss of hypothalamic hypocretin-producing neurons, resulting in severely disturbed sleep-wake control and cataplexy. Hypocretin-producing neurons project widely throughout the brain, influencing different neural networks. We assessed the extent of microstructural white matter organization and brain-wide structural connectivity abnormalities in a homogeneous group of twelve drug-free patients with narcolepsy type 1 and eleven matched healthy controls using diffusion tensor imaging with multimodal analysis techniques. First, tract-based spatial statistics (TBSS) was carried out using fractional anisotropy (FA) and mean, axial and radial diffusivity (MD, AD, RD). Second, quantitative analyses of mean FA, MD, AD and RD were conducted in predefined regions-of-interest, including sleep-wake regulation-related, limbic and reward system areas. Third, we performed hypothalamus-seeded tractography towards the thalamus, amygdala and midbrain. TBSS analyses yielded brain-wide significantly lower FA and higher RD in patients. Localized significantly lower FA and higher RD in the left ventral diencephalon and lower AD in the midbrain, were seen in patients. Lower FA was also found in patients in left hypothalamic fibers connecting with the midbrain. No significant MD and AD differences nor a correlation with disease duration were found. The brain-wide, localized ventral diencephalon (comprising the hypothalamus and different sleep- and motor-related nuclei) and hypothalamic connectivity differences clearly show a heretofore underestimated direct and/or indirect effect of hypocretin deficiency on microstructural white matter composition, presumably resulting from a combination of lower axonal density, lower myelination and/or greater axon diameter.

1. Introduction

Narcolepsy type 1 is a severely disabling neurological condition, characterised by excessive daytime sleepiness (EDS), attention deficits, cataplexy, sleep paralysis, hypnagogic hallucinations and disturbed nocturnal sleep. It has been suggested that it is an autoimmune-mediated disorder but the exact pathophysiology remains to be discovered (Liblau et al., 2015). Patients with narcolepsy type 1 show a selective loss of hypothalamic neurons producing hypocretin (or orexin) (Peyron et al., 2000; Thannickal et al., 2000). In an average healthy brain, each hemisphere comprises roughly 50,000–80,000 hypocretin-producing neurons, localized exclusively within the lateral and posterior hypothalamus (Moore et al., 2001). Their axonal projections diffusely disperse over the brain excluding the cerebellum with particularly dense projections to the locus coeruleus, ventral tegmental area and the tuberomammillary, raphe, laterodorsal tegmental and pedunclopontine tegmental nuclei (Sakurai, 2007). Hypocretin affects various neural networks; it maintains sleep-wake state stability, energy homeostasis, reward system regulation and cognitive and mood control (Nishino and Sakurai, 2005). Given the variety of complains in narcolepsy, a pertinent question is to what extent local and global white brain matter integrity and connectivity are affected.

DTI is an MRI technique enabling in-vivo modelling of microstructural white matter (WM) morphology by means of water diffusivity variations in different tissue types (Basser et al., 1994). Scalar variables of fractional anisotropy (FA) and mean, axial and radial diffusivity (MD,

* Corresponding author at: Department of Anatomy and Neurosciences, Amsterdam UMC (Location VUmc), De Boelelaan 1108, 1007 MB Amsterdam, the Netherlands.
E-mail addresses: J.gool@amsterdamumc.nl, j.k.gool@lumc.nl (J.K. Gool).

https://doi.org/10.1016/j.nicl.2019.101963
Received 3 April 2019; Received in revised form 20 June 2019; Accepted 26 July 2019
Available online 29 July 2019

AD, RD) are normally used as outcome measures. Fractional anisotropy (FA), reflects how directionally constrained the diffusion of water is along axons. While higher FA values might indicate more coherent, intact axons and/or higher myelination, lower FA may imply loss of WM integrity and/or injury. MD is composed of the mean diffusion in all three diffusion directions as a quantitative measure of alterations in the extracellular volume. AD captures the most prominent direction, parallel to axon orientation and RD the mean of the remaining perpendicular two directions. Lower AD reflects axonal damage, whereas higher RD is related to lower axonal density, lower myelination and/or greater axon diameter (Chanraud et al., 2010; Soares et al., 2013; Song et al., 2002). The outcome measures reflect the sum of different underlying tissue characteristics within one voxel. Possible differences are often explained by a combination of aforementioned morphological features.

Six diffusion tensor imaging (DTI) studies investigating structural WM morphology in people with narcolepsy compared to controls have previously been reported (Juvodden et al., 2018; Menzler et al., 2012; Nakamura et al., 2013; Park et al., 2016; Scherfler et al., 2012; Tezer et al., 2018). Findings are inconsistent, but disruptions were found in the hypothalamus–thalamus–orbitofrontal pathway and the brainstem as parts of the sleep-wake regulation system, as well as in the reward and limbic system and the corticospinal tract. The findings of previous DTI studies including patients with narcolepsy type 1 or narcolepsy with cataplexy are summarized in Supplementary Table I. Inconsistencies likely result from methodological differences between studies, including the use of central nervous system stimulants (Alicata et al., 2009), small groups, age variability (Giorgio et al., 2010), differences in patient characteristics (narcolepsy related to H1N1-vaccination, disease duration and severity) and restricted outcome measures (only FA and MD), making the interpretation complex.

Previous studies solely used whole-brain tract-based spatial statistics (TBSS) or whole-brain voxel-based morphometry (VBM) with diffusion metrics, which both are unable to assess interregional connectivity and compare regions subject to anatomical variation. Our aim was to identify the extent and nature of microstructural WM integrity disruptions in people with narcolepsy type 1 using a three-way analysis strategy, combining whole-brain TBSS **(I)**, region-of-interest (ROI) analyses **(II)** and tractography **(III).** Where TBSS identifies whole-brain microstructural WM differences within regions of considerable proportion, the ROI-based analyses also assess average microstructural WM integrity in regions with anatomical variability, while hypothalamus-seeded tractography specifically assesses the hypothalamic connectivity throughout the brain. Given the diversity in symptoms experienced by patients, we hypothesized that patients in comparison to controls in general show brain-wide lower FA, higher RD and unaffected MD **(I),** localized lower FA in symptom-related regions (e.g. ventral diencephalon, midbrain, thalamus) **(II)** and in hypothalamus-seeded tracts to the thalamus, amygdala and midbrain. **(III)**. In the TBSS analyses **(I)** we also expected significant relationships between longer disease durations, higher sleepiness scores and lower FA in regions related to the arousal system, including the pons, midbrain, thalamus and prefrontal cortex.

2. Materials and methods

2.1. Participants

Twelve adults with narcolepsy type 1 were recruited at our outpatient narcolepsy clinic (Sleep-Wake Centre SEIN) and eleven age and sex group-matched healthy controls were recruited through adverts in local newspapers. To be included, all subjects had to be 18–65 years old; right-handed according to the Edinburgh Handedness Scale (Oldfield, 1971) and have normal or corrected-to-normal vision. People with narcolepsy type 1 were diagnosed according to the 3rd edition of the International Classification of Sleep Disorders (American Academy of Sleep Medicine, 2014) and had to be treatment-naïve or off medication for ≥14 days prior to the study. Exclusion criteria consisted of current use of psychotropic drugs; current diagnosis of any other serious medical conditions; contraindications for MRI studies and macroscopic structural brain abnormalities (tumor, ventricle enlargement, cortical atrophy or vascular lesions).

In line with diagnostic criteria, the three patients without clear-cut cataplexy had hypocretin-1 levels determined in their cerebrospinal fluid (CSF). One patient had a concentration slightly higher (138 pg/mL) than the according to international standards assessed 110 pg/mL diagnostic threshold for narcolepsy type 1 (Mignot et al., 2002). This patient was still included because of the typical clinical phenotype and the still deficient hypocretin-1 level. All demographic and DTI analyses were repeated excluding this subject to verify that this person was no outlier. In total, CSF hypocretin-1 levels were available in nine patients as part of regular clinical care, of which all were hypocretin deficient. All patients had positive HLA-typing for DQB1*0602. Seven patients were drug naïve, and five discontinued their stimulants (4× methylphenidate and 1× modafinil) at least 2 weeks prior to study start. The five subjects had been using medication for 1–5 months prior to discontinuation.

Following subject screening to assess study eligibility, written informed consent was obtained from all subjects. The study protocol was approved by the Medical Ethical Committee of LUMC.

2.2. Data acquisition

All subjects completed a survey on general characteristics (e.g. age and previous medication use). In addition, the Dutch Adult Reading Test (Schmand et al., 1991) was completed to assess intelligence (IQ) and the Epworth Sleepiness Scale (ESS) (Johns, 1991) was administered as a measure of daytime sleepiness. All data collection was performed during the afternoon and subjects were asked to refrain from caffeine containing substances for at least 24 h prior to examination.

MRI data were acquired with a high-field 3 T Philips Achieva MRI scanner (Philips Healthcare, Best, the Netherlands) and a 32-channel head coil with sponge cushions to minimize head movements. Three-dimensional T1-weighted images (220 slices; TR 8.2 ms; TE 3.8 ms; inversion time 670.4 ms; FOV 240 × 240 × 220 mm; matrix size 240 × 240; flip angle 8°; 1 × 1 × 1 mm^3 voxel size) and single-shot, gradient-echo, echo-planar imaging (EPI) sequences for DTI (60 slices; TR = 6700 ms; TE = 72 ms; FOV 224 × 224 × 120 mm; matrix size 112 × 112; flip angle = 90°; 2 × 2 × 2 mm^3 voxel size) were obtained. DTI was carried out twice with reversed k-space readout along 46 non-collinear directions with b = 1000 s/$mm^2$and one unweighted b = 0 s/mm^2 image, each. Acquisition time was 6.2 min for T1-weighted scans and 5.9 min for each DTI scan.

One experienced reviewer (JKG), blinded to the scan identity, inspected the unprocessed T1-weigthed and DTI scans and processing steps as mentioned hereafter. Subcortical segmentations, cortical parcellations and the registration of ROIs to DTI subject space were additionally manually corrected if needed.

2.3. T1-weighted image processing

After visual examination of the T1-weighted images for artefacts and macroscopic brain abnormalities, the intensity was normalized and Freesurfer's MRI analysis software package (v5.3.0 Developmental) was used to automatically generate subcortical segmentations and cortical parcellations (Fischl et al., 2002; Iglesias et al., 2015).

ROIs were determined a priori on the basis of previously reported neuroimaging results (Supplementary Table I) and included regions likely related to narcolepsy complaints. All regions were part of the sleep-wake regulation, limbic or reward system and consisted of the hypothalamus, ventral diencephalon, thalamus, midbrain, amygdala, parahippocampal, anterior cingulate (merged rostral and caudal

anterior cingulate WM), medial and lateral orbitofrontal WM.

The hypothalamus was manually segmented in both hemispheres using standardized criteria (Nieuwenhuys et al., 1988). The anterior boundary of the hypothalamus consisted of the first coronal slice posterior of where the anterior commissure became discontinuous. Posteriorly, the last slice was where the mammillary bodies (included) diverted one another in the mid-sagittal plane. The hypothalamus inferiorly ended where the optic chiasm and infundibular stalk began and the anterior–posterior commissure plane was used for the superior delineation, which in itself was not included. Laterally, the segmentation was limited by WM of the internal capsule. Hypothalamus segmentation was blindly performed, twice for every subject. Corresponding maps were visually compared and combined to form the eventual segmentation.

2.4. Diffusion tensor image processing

After automatic brain extraction (Jenkinson et al., 2005), DTI scans were corrected for susceptibility-, eddy current- and subject movement-induced distortions with the FMRIB Software Library's (FSL, v5.0) topup and eddy tools (Andersson et al., 2003; Andersson and Sotiropoulos, 2016). Calculated off-resonance field maps were applied and 'dropout-slices' were replaced using non-parametric, Gaussian process modelled predictions (Andersson et al., 2016; Andersson and Sotiropoulos, 2016).

All ROIs were subsequently resampled to the corresponding pre-processed b0 images using linear coregistration of the T1-weighted image, to precisely identify subject-unique ROIs for local and tractography analyses. Incomplete imaging of an ROI due to incorrect field-of-view alignment resulted in the exclusion of this subject from the analyses including this ROI. The posterior-to-anterior-encoded DTI scan of one control subject was missing and therefore only the anterior-to-posterior-encoded images were used for this subject.

2.4.1. Tract-based spatial statistics (I)

In FSL's TBSS processing stream (Smith et al., 2006), the two DTI scans were averaged and projected onto an alignment-invariant skeleton image and thresholded at a > 0.2 FA level. All individual FA, MD, AD and RD maps were subsequently projected onto the skeleton, smoothed (5 mm) and fed into permutation-based voxelwise cross-subject statistics with 10,000 permutations and threshold-free cluster enhancement to identify between-group differences. The FA results were masked with FSL's JHU white matter tractography atlas' tracts (Hua et al., 2008) and presented as absolute and relative significant voxel ($p < .05$) counts with the corresponding minimum p-value. To verify robustness of the results, an additional TBSS FA analysis was done evenly mixing patients and controls by creating two randomly composed groups with a random number generator.

2.4.2. Region-of-interest analyses (II)

Pre-processed DTI images by FSL and predefined ROIs served as input for the volume-based pipeline of ExploreDTI's MATLAB-based MR diffusion toolbox (Leemans et al., 2009). B-matrix calculation and weighted linear least-squares estimators were used to calculate individual diffusion measure maps (FA and MD), that were subsequently masked with the personal ROIs in DTI subject space. The generated outcome measures were averaged for each subject's two DTI series and served as input for statistical analysis. ROI analyses were limited to only include FA and MD as we hypothesized that these summary measures would be most sensitive to detect underlying white matter differences and to limit the total number of comparisons. In case mean FA or MD were found to be significantly different in an ROI, post-hoc analyses were performed on AD and RD in these regions.

2.4.3. Tractography analyses (III)

Deterministic tractography was carried out using ExploreDTI's three-dimensional automated atlas-based tractography pipeline with a 0.2 FA threshold and maximum 30° angle change. Included fibers had to pass through the hypothalamus and a second pre-defined ROI (thalamus, amygdala or midbrain) in the corresponding hemisphere and not cross the midsagittal plane, except for the midbrain analyses. Tracts had to be within 10–200 mm length and only the segments between the ROIs were extracted to guarantee intersubject tract correspondence. More diffuse tracts connecting the hypothalamus with the orbitofrontal, anterior cingulate and parahippocampal WM were not found for every subject and were therefore not included in the eventual analyses. Total tract bundle volume and mean FA and MD results were automatically calculated in a voxel-by-voxel manner and served as input for statistical analysis.

As the visual inspection of the corrected b0 and FA images showed misalignment of several voxels in the hypothalamus between the scans with opposite phase-encoding directions, only the anterior-to-posterior-encoded DTI series was incorporated for tractography analyses as less deformity was seen.

2.5. Statistical analysis

Statistical processing of demographic, clinical and diffusion measures was done in IBM SPSS Statistics version 24, with p-values < .05 being considered as statistically significant. Student's t-tests were used for age, IQ and ESS comparisons between groups and a chi-square test to identify possible sex differences. Separate TBSS FA analyses were carried out in patients using time since EDS onset and ESS score as covariates of interest. Averaged ROI and tractography results were processed using one-way analyses of covariance (ANCOVAs). All DTI analyses were corrected for within group age and sex variability as covariates of no interest. Additional correction for whole-brain volume was performed in tractography analyses on absolute tract volume. Bonferroni correction for multiple comparisons was used per outcome measure for all ROI ($p < .0029$ for FA and MD and $p < .0125$ for AD and RD) and tractography ($p < .0083$) analyses.

3. Results

3.1. Demographic and clinical data

Data from age-and-sex-matched patients and controls were included in a 12:11 ratio. As shown in Table 1, there were no significant demographic and clinical differences between the groups, except for ESS score, which was higher in patients [10.08 ± 3.00 vs. 2.64 ± 1.96; $t(21) = -6.97$, $p < .001$]. The patient with a 1 38 pg/mL hypocretin-1 level was no outlier in any of the demographic or DTI analyses.

3.2. Tract-based spatial statistics (I)

Whole-brain microstructural WM differences were observed in people with narcolepsy in comparison to controls by means of overall significantly lower FA and higher RD (Fig. 1). Most prominent differences were found in the bilateral ventral diencephalon (comprising i.e. hypothalamus), thalamus, midbrain, pons, (orbito-) frontal, anterior cingulate, primary motor and somatosensory WM, internal capsule and the corpus callosum. No differences between groups were seen in other contrasts and in the cerebellum altogether. No significant relationships between time since EDS onset and ESS score and FA were present. Randomly creating two new groups pooling evenly cases and controls to detect spurious results did not yield significant differences.

Masking the FA results with the JHU white matter tractography atlas' tracts showed highly significant clusters with lower FA widely spread throughout the brain (Fig. 2); up to 68.1% of the left corticospinal tract voxels were significantly different. In contrast, only the parahippocampal cingulum WM showed a limited number of significantly different voxels [left: 2.1%, right: 3.3%].

Table 1
Characteristics of the study population.

	Patients (n = 12)	Controls (n = 11)	P-value
Male:female (N:N)	8:4	7:4	0.879
Age (years)			
Mean (SD)	33.25 (10.50)	31.82 (13.39)	0.777
Median (IQR)	32 (24.25–40.5)	26 (23–38.5)	
Range	21–52	18–55	
IQ score (mean, SD)	110.58 (10.73)	111.30 (8.25)	0.865
Age of onset EDS (years, mean, SD)	19.42 (9.15)	–	
EDS duration (years, median, IQR)	10.00 (6.00–25.25)	–	
Cataplexy presence	9/12	–	
Cataplexy and/or hypocretin deficient[a]	12/12	–	
HLA DQB1[a]0602 presence	12/12	–	
ESS score (mean, SD)	10.08 (3.00)	2.64 (1.96)	0.001
MSLT			
Sleep latency (minutes, mean, SD)	4.62 (3.64)	–	
SOREM periods (mean, SD)	2.58 (1.57)	–	
Polysomnography			
TST (minutes, mean, SD)	426.50 (25.33)	–	
Sleep efficiency (% of TST, mean, SD)	91.89 (5.49)	–	
Stage 1 sleep (% of TST, mean, SD)	12.75 (7.19)	–	
Stage 2 sleep (% of TST, mean, SD)	43.91 (10.38)	–	
Stage 3–4 sleep (% of TST, mean, SD)	17.40 (8.65)	–	
Stage REM sleep (% of TST, mean, SD)	23.86 (6.00)	–	
PLMI (mean, SD)	4.84 (7.50)	–	

EDS, excessive daytime sleepiness; ESS, Epworth sleepiness scale; HLA, human leukocyte antigen; MSLT, multi sleep latency test; PLMI, periodic leg movement index; SOREM, sleep onset rapid eye movement; TST, total sleep time.

[a] One patient had a deficient hypocretin-1 level (138 pg/mL) slightly above the diagnostic threshold (< 110 pg/mL). This patient was still included given the clinically typical narcolepsy and still deficient hypocretin-1 level.

3.3. Region-of-interest analyses (II)

As expected from the TBSS results, statistically significant lower FA was seen in patients (Table 2, Fig. 3) in the ventral diencephalon [left: $F(1,19) = 16{,}024$, $p = .001$; right: $F(1,19) = 6.604$, $p = .019$], left thalamus [$F(1,19) = 5.365$, $p = .032$] and midbrain [$F(1,19) = 4.394$, $p = .050$]. Patients also showed higher MD in the left ventral diencephalon [$F(1,19) = 5.511$, $p = .030$]. After Bonferroni correction for multiple comparisons ($p < .0029$) only the lower FA in the left ventral diencephalon maintained its significance. Post-hoc analyses on the bilateral ventral diencephalon, left thalamus and midbrain (Table 3) found significantly lower AD in the midbrain [$F(1,19) = 10.934$, $p = .004$] and significantly higher RD in the left ventral diencephalon [$F(1,19) = 8.722$, $p = .008$] in patients.

3.4. Tractography (III)

Statistically significant lower FA [$F(1,19) = 9.287$, $p = .007$] and lower tract volume [$F(1,18) = 5.256$, $p = .034$] were found in the WM tracts connecting the left hypothalamus with the midbrain (Table 4, Fig. 4). Only the lower FA maintained its significance after Bonferroni correction for multiple comparisons ($p < .0083$). No statistically significant differences were seen in MD. All fibers running through the hypothalamus are bilaterally visualized in Supplementary Video I for the same subject that is presented in Fig. 4.

4. Discussion

Microstructural WM properties were significantly abnormal in people with narcolepsy type 1 in the three methodologies used. Whole-brain lower FA and higher RD – excluding the cerebellum – were seen in people with narcolepsy type 1 within functional networks such as the sleep-wake regulation, limbic and reward system and corticospinal tract **(I)**. In patients mean lower FA and higher RD in the left ventral diencephalon and lower AD in the midbrain were found **(II)**. Patients' tracts connecting the left hypothalamus with the midbrain showed lower FA **(III)**. This study suggests a heretofore underestimated modulatory effect of hypocretin deficiency on microstructural white matter composition in patients with narcolepsy type 1.

4.1. Tract-based spatial statistics (I)

The widespread microstructural WM disruptions we found **(I)**, are generally in keeping with a previous large-scale TBSS study (Juvodden et al., 2018) which found brain-wide significantly lower FA and indifferent MD in drug-naïve patients with narcolepsy type 1, including the corpus callosum, midbrain and bilateral cingulate gyrus, thalamus, internal capsule. Higher RD was also reported in the midbrain and bilateral thalamus and lower AD in the corpus callosum. Discrepancies with this study in AD and RD differences most likely result from their lower disease duration (5.7 years) and the almost exclusive inclusion of patients that developed narcolepsy type 1 after H1N1-vaccination.

Similar results were also seen in two other TBSS studies (Park et al., 2016; Tezer et al., 2018) which reported selective extensively lower FA in patients with narcolepsy. Significant areas included the corpus callosum (the genu for Park et al., 2016 and body for Tezer et al., 2018), anterior internal capsule and thalamus. Tezer et al. (2018) additionally found lower FA in the midbrain, temporal lobe and cerebellum, whereas Park et al. (2016) also reported differences in the bilateral anterior cingulate, frontal lobe and left posterior internal capsule and thalamus. These regions were also found to be abnormal in our study, except for the cerebellum. This slight difference could be related to the absence of hypocretin measurements in these two studies and the lower b-values that were used for DTI acquisition, which are known to influence the diffusion metrics.

A fourth TBSS study (Menzler et al., 2012) reported both lower and higher FA in the right hypothalamus, brainstem, corticospinal tract and temporal, frontal and parietal WM. Inconsistencies with this latter study in FA disruption directions are possibly related to the use of psychotropic drugs (mostly central nervous system stimulants) in these patients compared to our drug-free population, as medication is known to influence WM morphology (Alicata et al., 2009).

Our results are in partial agreement with the whole-brain VBM-style study by Scherfler et al. (2012) that reported significantly lower FA and

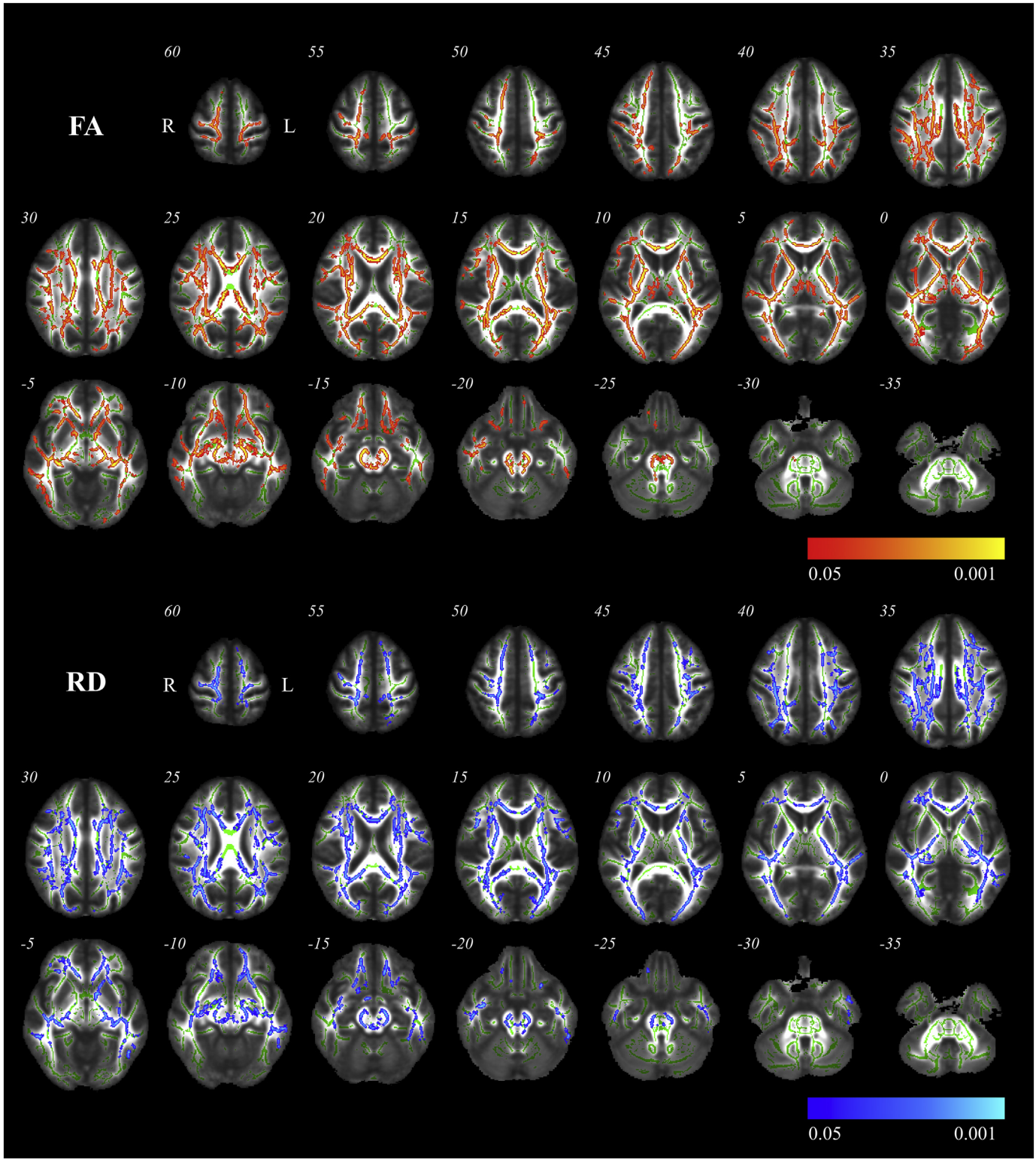

Fig. 1. Axial slices displaying significantly lower fractional anisotropy (FA) and higher radial diffusivity (RD) in patients with narcolepsy type 1 compared to controls. The average FA map of all subjects forms the background with the skeleton image of the included voxels (green) and the significantly different voxels (red-yellow) on top. Significant results are 1 mm inflated for visualization purposes. The numbers represent the corresponding axial slice in MNI152 space.

higher MD in the orbitofrontal cortex, anterior cingulate, singular lower MD in the ventral tegmental area, dorsal raphe nuclei and hypothalamus and lower FA measurements in the inferior frontal and inferior temporal cortices. Comparability with this study is difficult though, as included subjects on average were over 55 years of age and generally still used psychotropic medication. A second VBM study (Nakamura et al., 2013) has described increased MD in the left inferior frontal gyrus and left parahippocampal gyrus/amygdala and lower MD in the postcentral gyrus in narcolepsy with cataplexy patients compared to controls. Interestingly, the left laterization of amygdala differences that was reported by Nakamura et al. (2013) could not be replicated in this study as we found no significant differences in FA and MD in the left

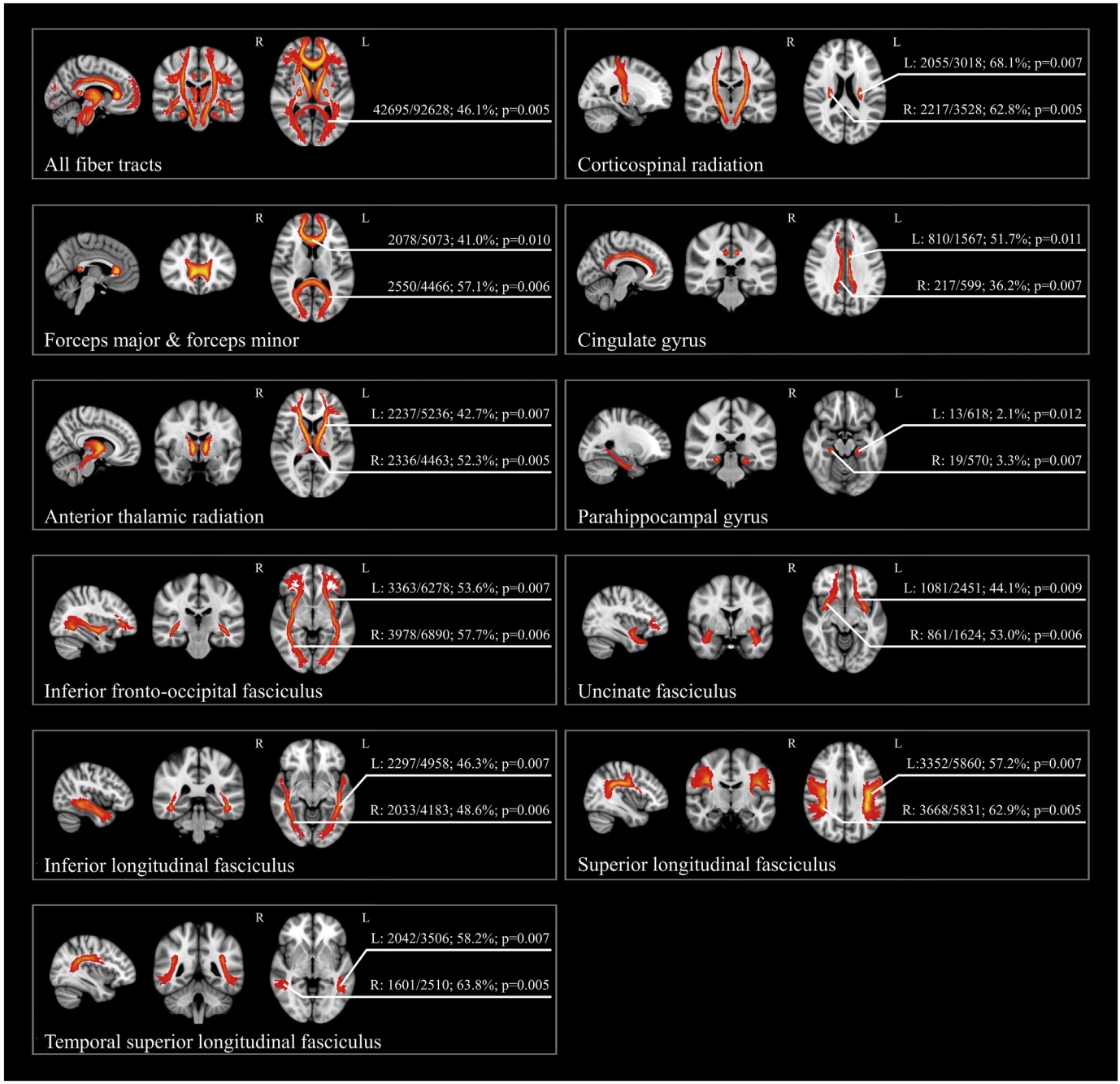

Fig. 2. The averaged FA map masked with the JHU tractography atlas labels (red-yellow). Reported as absolute significantly different voxel count within the label/total voxels within the label, corresponding percentage of significant voxels, minimum *p*-value found within the label.

amygdala in the ROI analyses. The reliability of these VBM-style approaches remains problematic given its susceptibility to bias from incorrect subject alignment and the inconsistent use of smoothing, making interpretability complex (Bookstein, 2001; Jones et al., 2005; Van Hecke et al., 2010). This could have especially affected the latter study due to its limited spatial resolution (3.5 mm voxel thickness) and the 12 mm smoothing that was used.

The brain-wide TBSS abnormalities excluding the cerebellum, are in concordance with previous histological findings on normal hypocretin projection patterns, as they describe whole-brain axonal branching of hypocretin-expressing neurons from the hypothalamus, except for the cerebellum (Sakurai, 2007). We take the absence of WM differences in the cerebellum, the absence of significant differences after the control TBSS analysis with randomized groups, and the specific significance in only the lower FA and higher RD contrasts as a sign of the robustness of our results.

4.2. Region-of-interest analyses (II)

In the ROI analyses, lower FA was found in patients, especially in the highly significant left ventral diencephalon. In the post-hoc analyses, significantly higher RD was also found in this region in addition to significantly lower AD in the midbrain. **(II)**. The ventral diencephalon is filled with a variety of sleep-wake regulation areas, including those in the hypothalamus and superior midbrain. Other included regions are related to motor functioning and the reward system, such as the subthalamic nucleus, substantia nigra and red nucleus and connecting fibers of the crus cerebri, lenticular fasciculus and medial

Table 2
Region-of-interest FA and MD analyses.

	Fractional anisotropy			Mean diffusivity		
	Patients (mean, SD)	Controls (mean, SD)	P-value	Patients (mean, SD)	Controls (mean, SD)	P-value
Left thalamus	0.370 (0.015)	0.387 (0.020)	0.032	0.755 (0.020)	0.745 (0.019)	0.229
Right thalamus	0.348 (0.013)	0.360 (0.015)	0.061	0.785 (0.018)	0.788 (0.029)	0.746
Left amygdala	0.245 (0.017)	0.244 (0.027)	0.942	0.811 (0.017)	0.807 (0.027)	0.614
Right amygdala	0.240 (0.017)	0.238 (0.013)	0.897	0.838 (0.021)	0.848 (0.040)	0.499
Left ventral diencephalon	0.489 (0.016)	0.521 (0.021)	0.001	0.846 (0.061)	0.799 (0.042)	0.030
Right ventral diencephalon	0.482 (0.017)	0.506 (0.028)	0.019	0.866 (0.043)	0.834 (0.056)	0.129
Left hypothalamus	0.293 (0.026)	0.299 (0.026)	0.483	1.144 (0.127)	1.328 (0.399)	0.165
Right hypothalamus	0.280 (0.021)	0.292 (0.026)	0.186	1.210 (0.128)	1.209 (0.209)	0.968
Left lateral orbitofrontal WM	0.393 (0.020)	0.401 (0.020)	0.301	0.751 (0.025)	0.741 (0.017)	0.287
Right lateral orbitofrontal WM	0.397 (0.021)	0.401 (0.018)	0.588	0.740 (0.029)	0.731 (0.022)	0.430
Left medial orbitofrontal WM	0.368 (0.024)	0.376 (0.030)	0.359	0.750 (0.032)	0.743 (0.020)	0.612
Right medial orbitofrontal WM	0.385 (0.028)	0.397 (0.033)	0.368	0.767 (0.020)	0.770 (0.026)	0.738
Left anterior cingulate WM	0.535 (0.025)	0.534 (0.023)	0.921	0.768 (0.039)	0.769 (0.034)	1.000
Right anterior cingulate WM	0.557 (0.024)	0.566 (0.038)	0.365	0.803 (0.031)	0.814 (0.032)	0.457
Left parahippocampal WM	0.413 (0.008)	0.420 (0.032)	0.391	0.786 (0.014)	0.779 (0.034)	0.550
Right parahippocampal WM	0.419 (0.018)	0.422 (0.028)	0.604	0.803 (0.027)	0.803 (0.035)	1.000
Midbrain	0.530 (0.058)	0.575 (0.018)	0.050*	1.038 (0.121)	1.119 (0.077)	0.086

WM, white matter.
* Unrounded p-value = .049693.

lemniscus. The lower AD in the midbrain indicates axonal loss in patients (Wheeler-Kingshott and Cercignani, 2009) and could be explained by the loss of hypothalamic projections running through the midbrain towards sleep-wake-, motor- and reward-regulating nuclei in the brainstem, including the ventral tegmental area, locus coeruleus and laterodorsal tegmental, raphe and pedunculopontine tegmental nuclei (Sakurai, 2007). The ROI findings further validate the correspondence between WM integrity disruptions in patients with narcolepsy and sleep-wake, reward system and motor complaints.

4.3. Tractography analyses (III)

Although not always significant, the overall lower FA and generally lower volume of patients' tracts indicate a correlation between hypocretin deficiency and WM integrity disruptions in fiber bundles connecting with the hypothalamus, especially passing through the

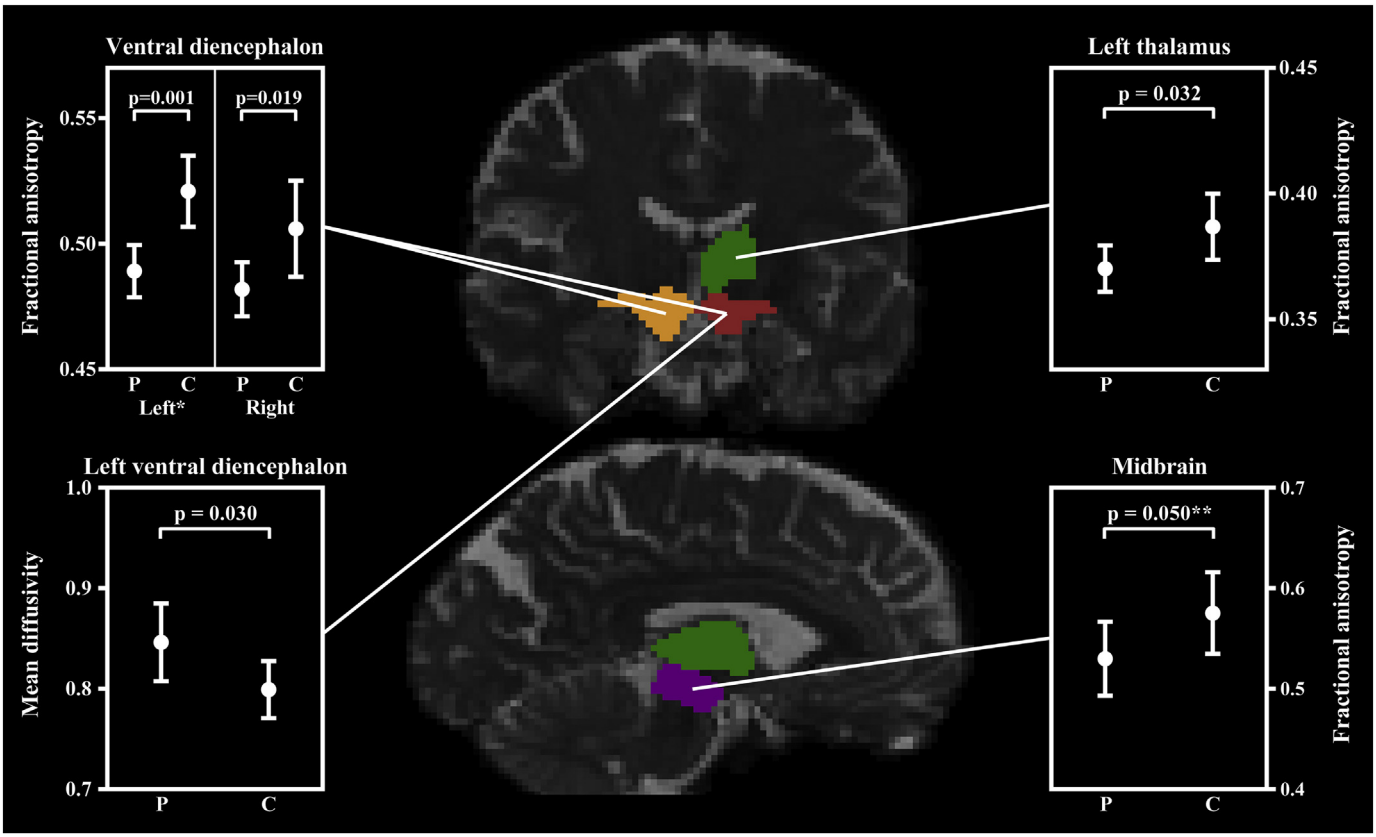

Fig. 3. The significant ROIs displayed in native space of one subject, for visualization purposes. The mean (and 95% confidence interval) FA and MD values are plotted for patients (P) and controls (C) separately with the corresponding p-value on top. The unrounded *p*-value for the midbrain was $p = .049693$ (**). After Bonferroni correction for multiple comparisons only the left ventral diencephalon (*) maintained significant.

Table 3
Post-hoc region-of-interest AD and RD analyses.

	Axial diffusivity			Radial diffusivity		
	Patients (mean, SD)	Controls (mean, SD)	P-value	Patients (mean, SD)	Controls (mean, SD)	P-value
Left thalamus	1.061 (0.023)	1.063 (0.013)	0.766	0.602 (0.021)	0.587 (0.025)	0.106
Left ventral diencephalon	1.330 (0.090)	1.298 (0.047)	0.225	0.604 (0.049)	0.550 (0.043)	0.008
Right ventral diencephalon	1.357 (0.070)	1.330 (0.056)	0.307	0.621 (0.035)	0.586 (0.060)	0.097
Midbrain	1.735 (0.183)	1.924 (0.701)	0.004	0.690 (0.012)	0.717 (0.010)	0.614

midbrain **(III)**. No direct comparison of these results could be made as this is the first tractography study in people with narcolepsy. Our reported overall projection pattern is in line with previous hypothalamic tractography results (Lemaire et al., 2011), where dense projections were found in healthy subjects to the thalamus, amygdala, parahippocampus and brainstem and cortically widespread bundles mainly to the central gyri, frontal and occipital lobe. Our study found dense tracts connecting the hypothalamus with the thalamus, amygdala and midbrain in all subjects, whereas more diffuse connections were often seen to the orbitofrontal and parahippocampal WM. Tracts towards the anterior cingulate WM were less prevalent. Connections to other, not mentioned regions were out of this study's scope. The reason why more diffuse tracts are sometimes not detected when using tractography, is related to the partial volume effect. The contribution of diffuse tracts to the overall diffusion measures of a voxel is only marginal when the voxel also contains more dense tracts, resulting in loss of information (Assaf and Pasternak, 2008). Future research with increased spatial resolution and higher b-values could resolve this.

4.4. Interpretation

The exact origin of the WM differences remains unexplained, but previous research (Song et al., 2002; Wheeler-Kingshott and Cercignani, 2009) has suggested that lower FA and higher RD results from a combination of lower axonal density, lower myelination and/or greater axon diameter within affected areas. The extent of the observed abnormalities implies that narcolepsy type 1 is a brain-wide disorder not just limited to the hypothalamus. Considering the relatively limited 50,000–80,000 hypocretin-producing neurons normally present (Moore et al., 2001), these results suggest a more complex pathway causing the WM abnormalities in patients, presumably not directly caused by hypocretin deficiency. Involvement of a secondary mechanism or the presence of a cascade of alterations related to hypocretin deficiency seems likely. A similar pathophysiology has been suggested by Juvodden et al. (2018). The limited significant differences in the studied connections passing through the hypothalamus further contradicts that the observed differences are solely of hypothalamic origin. In fact, it implies that narcolepsy type 1 is a brain-wide disorder, not just limited to the hypothalamus. We believe that future research should focus on this possible cascade of indirect effects, or parallel to, related to hypocretin deficiency as this could also give insight in the pathophysiology of different symptoms experienced by patients. It could also explain the susceptibility of patients to develop certain symptoms.

The absence a significant correlation between time since symptom onset and FA was unexpected. Similar results were previously seen (Juvodden et al., 2018; Park et al., 2016) and might be due to the relative end-stage narcolepsy in all studies. This indicated that when the chronic narcolepsy state has been reached, the brain reaches structural end-stage white matter composition. A comparison between patients in different disease stages, implementing a multimodal analysis strategy, should be the target of future research.

4.5. Methodological strengths and limitations

We assessed a homogeneous group of patients using a multimodal analysis strategy, to improve data quality and interpretability. All controls were age- and sex-matched and a standardized data acquisition and a three-way analysis strategy were used. By also adding RD and AD to the outcome measures, this study fills an important gap in the current literature as a more in-depth interpretation of the origin of the differences is included.

The relatively sporadic significance in the ROI-based **(II)** and tractography analyses **(III)** – compared to the widely present TBSS abnormalities – could mainly be attributed to intrinsic methodological differences, as averaging outcome measures within and between ROIs omits significant subregions, while TBSS **(I)** identifies subtler per-voxel differences (Mukherjee et al., 2008). The effect of crossing fibers and the relatively low proportion of hypocretin-producing neurons within the fiber bundles they follow, could further explain this. However, TBSS **(I)** is incapable of providing information on interregional connectivity and regions subject to anatomical variability as only regions containing dense white matter bundles are included (Bach et al., 2014). This could also explain the combination of significantly lower AD in patients in the midbrain in the ROI-based analyses **(II)** and the absence of significant AD differences in the TBSS results **(I)**. Given the distinct strengths and limitations of the individual methods and as previously suggested by Wakana et al. (2007), we would recommend standard implementation of combined analysis techniques for future research.

Although findings are robust, some limitations of our study also need to be addressed. An important limitation to the presented study is the limited sample size that was included. Future research should

Table 4
Hypothalamic white matter connectivity.

	Fractional anisotropy			Mean diffusivity			Tract volume[a]		
	Patients	Controls	P-value	Patients	Controls	P-value	Patients	Controls	P-value
Left – left thalamus	0.411 (0.033)	0.426 (0.022)	0.229	0.900 (0.085)	0.842 (0.075)	0.127	1.909 (0.753)	1.897 (0.760)	0.991
Right – right thalamus	0.412 (0.038)	0.430 (0.027)	0.191	0.918 (0.078)	0.911 (0.074)	0.814	2.017 (1.148)	2.052 (1.044)	0.745
Left – left amygdala	0.426 (0.050)	0.438 (0.045)	0.319	0.846 (0.115)	0.796 (0.058)	0.222	0.773 (0.324)	0.799 (0.392)	0.850
Right – right amygdala	0.399 (0.053)	0.418 (0.044)	0.239	0.940 (0.138)	0.849 (0.064)	0.058	0.782 (0.305)	0.873 (0.461)	0.560
Left – midbrain	0.419 (0.031)	0.458 (0.030)	0.007	0.782 (0.108)	0.758 (0.085)	0.512	2.156 (0.912)	2.894 (0.890)	0.034
Right - midbrain	0.405 (0.035)	0.428 (0.041)	0.130	0.868 (0.134)	0.861 (0.062)	0.845	2.395 (1.540)	3.595 (1.468)	0.079

Each row represents the tracts connecting the left or right hypothalamus with the mentioned ROI. Values are reported as mean (SD).
[a] Tract volume is in cm^3.

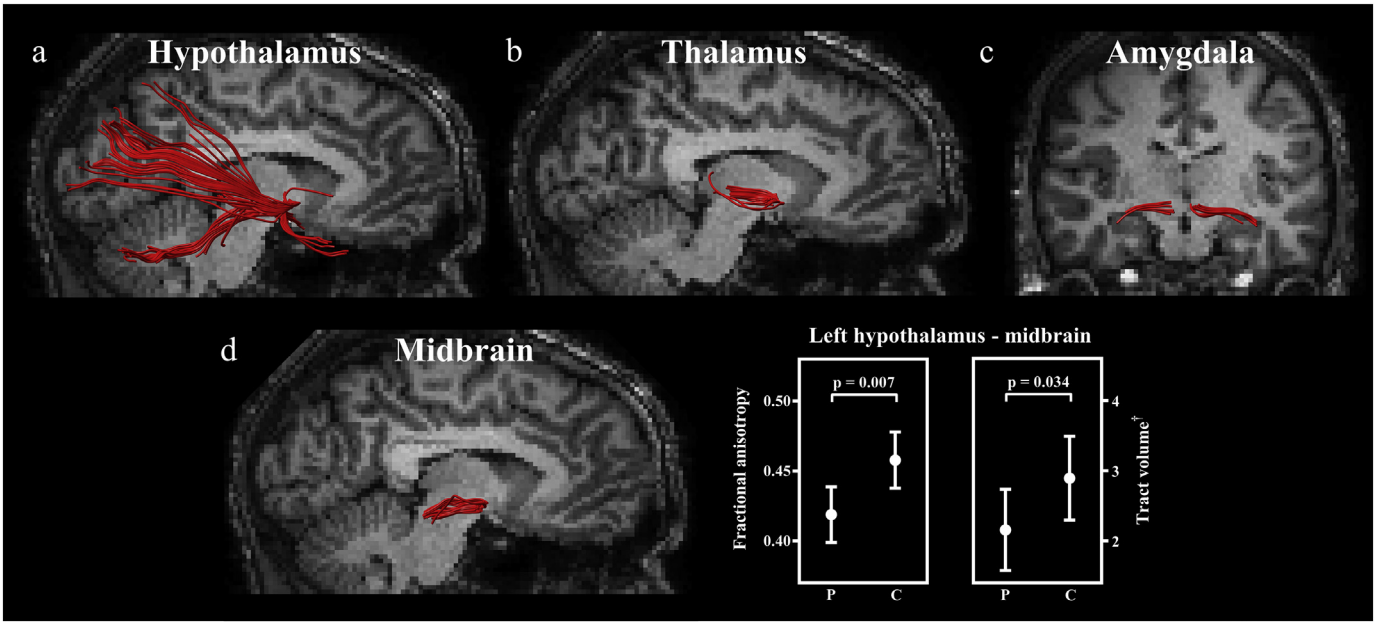

Fig. 4. Connectivity of the hypothalamus of one subject. In **A** the overall connectivity of the hypothalamus by itself is shown. **B-D** represent components of **A**, connecting the hypothalamus with the ROIs. Significantly different FA values were plotted as mean with the corresponding 95% confidence interval for both patients (P) and controls (C).

include larger samples to enable reliable subgroup analyses investigating the relationship between the presence of narcolepsy-related symptoms, neuropsychological measures, and the observed microstructural white matter abnormalities of patients with narcolepsy. Additionally, five patients had used psychotropic medication before inclusion. Even though medication was discontinued, this could have influenced results.

It should also be noted that the ventral diencephalon is a more reliable ROI than the hypothalamus for the ROI analyses, as this last region is particularly susceptible to CSF contamination and hence to partial volume artefacts. This is less relevant for tractography analyses, as a result of the used FA threshold.

5. Conclusion

The reported whole-brain **(I)**, localized ROI **(II)** and connectivity **(III)** differences clearly show lower FA in patients with narcolepsy compared to controls. In combination with the TBSS results showing brain-wide higher RD, this would indicate that narcolepsy type 1 patients suffer from a combination of lower axonal density, lower myelination and/or greater axon diameter (Song et al., 2002; Wheeler-Kingshott and Cercignani, 2009). Given the extent of the WM abnormalities, our results indicate a more complex cascade or a secondary pathway causing these differences, not solely explained by hypocretin deficiency on its own.

Supplementary data to this article can be found online at https://doi.org/10.1016/j.nicl.2019.101963.

Funding source declaration

This project has been sponsored by Leiden University Fund / Den Dulk-Moermans Fund. The funding sources was not involved in study design; the collection, analysis and interpretation of data; in the writing of the report or in the decision to submit the article for publication.

Declaration of Competing Interest

The authors would like to thank Sophie Schwartz, Aad Pors and Bo Scheffer for their help in scanning protocol composition and data acquisition. No conflicts of interest were present.

References

Alicata, D., Chang, L., Cloak, C., Abe, K., Ernst, T., 2009. Higher diffusion in striatum and lower fractional anisotropy in white matter of methamphetamine users. Psychiatry Res. 174, 1–8. https://doi.org/10.1016/j.pscychresns.2009.03.011.

American Academy of Sleep Medicine, 2014. European sleep research society. In: The International Classification of Sleep Disorders – Third Edition (ICSD-3). American Academy of Sleep Medicine, Darien, IL.

Andersson, J.L.R., Sotiropoulos, S.N., 2016. An integrated approach to correction for off-resonance effects and subject movement in diffusion MR imaging. NeuroImage 125, 1063–1078. https://doi.org/10.1016/j.neuroimage.2015.10.019.

Andersson, J.L., Skare, S., Ashburner, J., 2003. How to correct susceptibility distortions in spin-echo echo-planar images: application to diffusion tensor imaging. NeuroImage 20, 870–888. https://doi.org/10.1016/s1053-8119(03)00336-7.

Andersson, J.L.R., Graham, M.S., Zsoldos, E., Sotiropoulos, S.N., 2016. Incorporating outlier detection and replacement into a non-parametric framework for movement and distortion correction of diffusion MR images. NeuroImage 141, 556–572. https://doi.org/10.1016/j.neuroimage.2016.06.058.

Assaf, Y., Pasternak, O., 2008. Diffusion tensor imaging (DTI)-based white matter mapping in brain research: a review. J. Mol. Neurosci. 34, 51–61. https://doi.org/10.1007/s12031-007-0029-0.

Bach, M., Laun, F.B., Leemans, A., Tax, C.M.W., Biessels, G.J., Stieltjes, B., Maier-Hein, K.H., 2014. Methodological considerations on tract-based spatial statistics (TBSS). Neuroimage 100, 358–369. https://doi.org/10.1016/j.neuroimage.2014.06.021.

Basser, P.J., Mattiello, J., Lebihan, D., 1994. MR diffusion tensor spectroscopy and imaging. Biophys. J. 66, 259–267. https://doi.org/10.1016/S0006-3495(94)80775-1.

Bookstein, F.L., 2001. "Voxel-based Morphometry" should not be used with imperfectly registered images. Neuroimage 14 (6), 1454–1462. https://doi.org/10.1006/nimg.2001.0770.

Chanraud, S., Zahr, N., Sullivan, E.V., Pfefferbaum, A., 2010. MR diffusion tensor imaging: a window into white matter integrity of the working brain. Neuropsychol. Rev. 20 (2), 209–225. https://doi.org/10.1007/s11065-010-9129-7.

Fischl, B., Salat, D.H., Busa, E., Albert, M., Dieterich, M., Haselgrove, C., ... Dale, A.M., 2002. Whole brain segmentation: automated labeling of neuroanatomical structures in the human brain. Neuron 33, 341–355. https://doi.org/10.1016/S0896-6273(02)00569-X.

Giorgio, A., Santelli, L., Tomassini, V., Bosnell, R., Smith, S., De Stefano, N., Johansen-Berg, H., 2010. Age-related changes in grey and white matter structure throughout adulthood. NeuroImage 51, 943–951. https://doi.org/10.1016/j.neuroimage.2010.03.004.

Hua, K., Zhang, J., Wakana, S., Jiang, H., Li, X., Reich, D.S., ... Mori, S., 2008. Tract probability maps in stereotaxic spaces: analyses of white matter anatomy and tract-specific quantification. NeuroImage 39, 336–347. https://doi.org/10.1016/j.neuroimage.2007.07.053.

Iglesias, J.E., Van Leemput, K., Bhatt, P., Casillas, C., Dutt, S., Schuff, N., ... Alzheimer's Disease Neuroimaging Initiative, 2015. Bayesian segmentation of brainstem structures in MRI. NeuroImage 113, 184–195. https://doi.org/10.1016/j.neuroimage.

2015.02.065.
Jenkinson, M., Pechaud, M., Smith, S., 2005. BET2: MR-based estimation of brain, skull and scalp surfaces. In: Eleventh Annual Meeting of the Organization for Human Brain Mapping.
Johns, M.W., 1991. A new method for measuring daytime sleepiness: the Epworth sleepiness scale. Sleep 14, 540–545. https://doi.org/10.1093/sleep/14.6.540.
Jones, D.K., Symms, M.R., Cercignani, M., Howard, R.J., 2005. The effect of filter size on VBM analyses of DT-MRI data. Neuroimage 26, 546–554. https://doi.org/10.1016/j.neuroimage.2005.02.013.
Juvodden, H.T., Alnæs, D., Lund, M.J., Agartz, I., Andreassen, O.A., Dietrichs, E., ... Knudsen, S., 2018. Widespread white matter changes in post-H1N1 patients with narcolepsy type 1 and first-degree relatives. Sleep 41 (10), 1–11. https://doi.org/10.1093/sleep/zsy145.
Leemans, A., Jeurissen, B., Sijbers, J., Jones, D.K., 2009. ExploreDTI: a graphical toolbox for processing, analyzing, and visualizing diffusion MR data. In: Proceedings of the International Society for Magnetic Resonance in Medicine. vol. 17. pp. 3536.
Lemaire, J.J., Frew, A.J., McArthur, D., Gorgulho, A.A., Alger, J.R., Salomon, N., ... De Salles, A.A., 2011. White matter connectivity of human hypothalamus. Brain Res. 1371, 43–64. https://doi.org/10.1016/j.brainres.2010.11.072.
Liblau, R.S., Vassalli, A., Seifinejad, A., Tafti, M., 2015. Hypocretin (orexin) biology and the pathophysiology of narcolepsy with cataplexy. Lancet Neurol. 14 (3), 318–328. https://doi.org/10.1016/S1474-4422(14)70218-2.
Menzler, K., Belke, M., Unger, M.M., Ohletz, T., Keil, B., Heverhagen, J.T., ... Knake, S., 2012. DTI reveals hypothalamic and brainstem white matter lesions in patients with idiopathic narcolepsy. Sleep Med. 13, 736–742. https://doi.org/10.1016/j.sleep.2012.02.013.
Mignot, E., Lammers, G.J., Ripley, B., Okun, M., Nevsimalova, S., Overeem, S., ... Nishino, S., 2002. The role of cerebrospinal fluid hypocretin measurement in the diagnosis of narcolepsy and other hypersomnias. Arch. Neurol. 59, 1553–1562. https://doi.org/10.1001/archneur.59.10.1553.
Moore, R.Y., Abrahamson, E.A., Van Den Pol, A., 2001. The hypocretin neuron system: an arousal system in the human brain. Arch. Ital. Biol. 139, 195–205.
Mukherjee, P., Chung, S.W., Berman, J.I., Hess, C.P., Henry, R.G., 2008. Diffusion tensor MR imaging and fiber tractography: technical considerations. Am. J. Neuroradiol. 29 (5), 843–852. https://doi.org/10.3174/ajnr.A1052.
Nakamura, M., Nishida, S., Hayashida, K., Ueki, Y., Dauvilliers, Y., Inoue, Y., 2013. Differences in brain morphological findings between narcolepsy with and without cataplexy. PLoS One 8, e81059. https://doi.org/10.1371/journal.pone.0081059.
Nieuwenhuys, R., Voogd, J., Van Huijzen, C., 1988. The Human Central Nervous System: A Synopsis and Atlas. Springer-Verlag, Berlin, Germany. https://doi.org/10.1007/978-3-662-02333-4.
Nishino, S., Sakurai, T., 2005. The Orexin/Hypocretin System: Physiology and Pathophysiology. Humana Press, Otowa, NJ. https://doi.org/10.1385/1592599508.
Oldfield, R.C., 1971. The assessment and analysis of handedness: the Edinburgh inventory. Neuropsychologia 9, 97–113. https://doi.org/10.1016/0028-3932(71)90067-4.
Park, Y.K., Kwon, O.H., Joo, E.Y., Kim, J.H., Lee, J.M., Kim, S.T., Hong, S.B., 2016. White matter alterations in narcolepsy patients with cataplexy: tract-based spatial statistics. J. Sleep Res. 25, 181–189. https://doi.org/10.1111/jsr.12366.
Peyron, C., Faraco, J., Rogers, W., Ripley, B., Overeem, S., Charnay, Y., ... Mignot, E., 2000. A mutation in a case of early onset narcolepsy and a generalized absence of hypocretin peptides in human narcoleptic brains. Nat. Med. 6 (9), 991–997. https://doi.org/10.1038/79690.
Sakurai, T., 2007. The neural circuit of orexin (hypocretin): maintaining sleep and wakefulness. Nat. Rev. Neurosci. 8, 171–181. https://doi.org/10.1038/nrn2092.
Scherfler, C., Frauscher, B., Schocke, M., Nocker, M., Gschliesser, V., Ehrmann, L., ... Hogl, B., 2012. White and gray matter abnormalities in narcolepsy with cataplexy. Sleep 35, 345–351. https://doi.org/10.5665/sleep.1692.
Schmand, B., Bakker, D., Saan, R., Louman, J., 1991. The Dutch Reading Test for Adults: a measure of premorbid intelligence level. Tijdschr. Gerontol. Geriatr. 22, 15–19.
Smith, S.M., Jenkinson, M., Johansen-Berg, H., Rueckert, D., Nichols, T.E., Mackay, C.E., ... Behrens, T.E., 2006. Tract-based spatial statistics: voxelwise analysis of multi-subject diffusion data. NeuroImage 31, 1487–1505. https://doi.org/10.1016/j.neuroimage.2006.02.024.
Soares, J.M., Marques, P., Alves, V., Sousa, N., 2013. A hitchhiker's guide to diffusion tensor imaging. Front. Neurosci. 7, 31. https://doi.org/10.3389/fnins.2013.00031.
Song, S.K., Sun, S.W., Ramsbottom, M.J., Chang, C., Russell, J., Cross, A.H., 2002. Dysmyelination revealed through MRI as increased radial (but unchanged axial) diffusion of water. NeuroImage 17, 1429–1436. https://doi.org/10.1006/nimg.2002.1267.
Tezer, F.I., Erdal, A., Gumusyayla, S., Has, A.C., Gocmen, R., Oguz, K.K., 2018. Differences in diffusion tensor imaging changes between narcolepsy with and without cataplexy. Sleep Med. 52, 128–133. https://doi.org/10.1016/j.sleep.2018.08.022.
Thannickal, T.C., Moore, R.Y., Nienhuis, R., Ramanathan, L., Gulyani, S., Aldrich, M., ... Siegel, J.M., 2000. Reduced number of hypocretin neurons in human narcolepsy. Neuron 27 (3), 469–474. https://doi.org/10.1016/S0896-6273(00)00058-1.
Van Hecke, W., Leemans, A., De Backer, S., Jeurissen, B., Parizel, P.M., Sijbers, J., 2010. Comparing isotropic and anisotropic smoothing for voxel-based DTI analyses: a simulation study. Hum. Brain Mapp. 31, 98–114. https://doi.org/10.1002/hbm.20848.
Wakana, S., Caprihan, A., Panzenboeck, M.M., Fallon, J.H., Perry, M., Gollub, R.L., 2007. Reproducibility of quantitative tractography methods applied to cerebral white matter. Neuroimage 36 (3), 630–644. https://doi.org/10.1016/j.neuroimage.2007.02.049.
Wheeler-Kingshott, C.A., Cercignani, M., 2009. About "axial" and "radial" diffusivities. Magn. Reson. Med. 61, 1255–1260. https://doi.org/10.1002/mrm.21965.